Supplementary Material (ESI) for Inorganic Chemistry Frontiers
This journal is © The Royal Society of Chemistry

Assembly, Structures, Photophysical Properties and Photocatalytic Activities of a Series of Coordination Polymers Constructed from Semi-rigid Bis-pyridyl-bis-amide and Benzenetricarboxylic acid

Xiu-Li Wang*, Mao Le, Hong-Yan Lin, Jian Luan, Guo-Cheng Liu, Fang-Fang Sui, Zhi-Han Chang

Department of Chemistry, Bohai University, Liaoning Province Silicon Materials Engineering Technology Research Centre, Jinzhou 121000, P. R. China

Table S1. Selected bond distances (Å) and angles (°) for complex **1**

Co(1)−O(5)#1	2.024(2)	Co(1)−O(2)	2.118(3)
Co(1)−N(1)	2.046(2)	Co(1)−O(1)	2.236(3)
Co(1)−N(2)#2	2.056(2)	N(1)−Co(1)−O(1)	90.92(9)
O(5)#1−Co(1)−N(1)	104.86(9)	N(2)#2−Co(1)−O(1)	88.47(10)
O(5)#1−Co(1)−N(2)#2	126.05(10)	O(2)−Co(1)−O(1)	58.37(11)
N(1)−Co(1)−N(2)#2	103.48(9)	N(2)#2−Co(1)−O(2)	100.35(13)
O(5)#1−Co(1)−O(2)	85.48(9)	O(5)#1−Co(1)−O(1)	135.33(11)
N(1)−Co(1)−O(2)	140.31(15)		

Symmetry code: #1 $x, y + 1, z$; #2 $-x + 1/2, y + 1/2, -z - 1/2$

Table S2. Selected bond distances (Å) and angles (°) for complex **2**

Ni(1)−O(1)	2.0375(18)	Ni(1)−N(1)	2.113(2)
Ni(1)−O(2W)	2.069(2)	Ni(1)−N(3)	2.135(3)
Ni(1)−O(1W)	2.107(2)	Ni(1)−N(2)#1	2.158(2)
O(1)−Ni(1)−O(2W)	173.71(8)	O(1W)−Ni(1)−N(3)	97.11(13)
O(1)−Ni(1)−O(1W)	90.17(8)	N(1)−Ni(1)−N(3)	87.91(13)

* Corresponding author. Tel.: +86-416-3400158

E-mail address: wangxiuli@bhu.edu.cn (X.-L. Wang)

O(2W)−Ni(1)−O(1W)	83.55(8)	O(1)−Ni(1)−N(2)#1	92.35(9)
O(1)−Ni(1)−N(1)	91.18(8)	O(2W)−Ni(1)−N(2)#1	87.24(9)
O(2W)−Ni(1)−N(1)	95.05(8)	O(1W)−Ni(1)−N(2)#1	88.40(9)
O(1W)−Ni(1)−N(1)	174.79(9)	N(1)−Ni(1)−N(2)#1	86.52(9)
O(1)−Ni(1)−N(3)	90.30(11)	N(3)−Ni(1)−N(2)#1	173.88(11)
O(2W)−Ni(1)−N(3)	90.73(12)		

Symmetry code: #1 $-x-1, -y+1, -z$

Table S3. Selected bond distances (Å) and angles (°) for complex **3**

Cu(1)−O(1)	1.906(2)	Cu(1)−N(2)#2	2.013(3)
Cu(1)−O(3)#1	2.008(2)	Cu(1)−O(4)#1	2.371(2)
Cu(1)−N(1)	2.009(3)	O(3)#1−Cu(1)−O(4)#1	59.41(8)
O(1)−Cu(1)−O(3)#1	156.52(10)	N(1)−Cu(1)−O(4)#1	99.98(10)
O(1)−Cu(1)−N(1)	94.19(11)	N(2)#2−Cu(1)−O(4)#1	102.49(10)
O(3)#1−Cu(1)−N(1)	91.38(10)	N(1)−Cu(1)−N(2)#2	154.79(11)
O(1)−Cu(1)−N(2)#2	94.23(11)	O(1)−Cu(1)−O(4)#1	97.13(9)
O(3)#1−Cu(1)−N(2)#2	90.28(10)		

Symmetry code: #1 $x, y-1, z$; #2 $x-1/2, -y-1/2, z-1/2$

Table S4. Selected bond distances (Å) and angles (°) for complex **4**

Zn(1)−O(5)#1	1.9782(15)	Zn(1)−N(2)	2.0222(19)
Zn(1)−O(2)	1.9785(16)	Zn(1)−N(1)	2.046(2)
O(5)#1−Zn(1)−O(2)	96.71(7)	O(5)#1−Zn(1)−N(1)	116.67(7)
O(5)#1−Zn(1)−N(2)	106.53(7)	O(2)−Zn(1)−N(1)	105.34(7)
O(2)−Zn(1)−N(2)	127.98(8)	N(2)−Zn(1)−N(1)	104.45(8)

Symmetry code: #1 $x, y-1, z$

Table S5. Selected bond distances (Å) and angles (°) for complex **5**

Cd(1)−O(5)#1	2.3091(16)	Cd(1)−O(2)	2.4050(16)

Cd(1)−N(1)	2.3303(18)	Cd(1)−O(1)	2.5512(16)
Cd(1)−N(2)	2.3470(19)	Cd(1)−O(6)#1	2.5756(16)
Cd(1)−O(1W)	2.3655(16)	O(5)#1−Cd(1)−N(1)	139.63(6)
O(5)#1−Cd(1)−N(2)	90.27(7)	N(1)−Cd(1)−O(1)	84.17(6)
N(1)−Cd(1)−N(2)	95.47(7)	N(2)−Cd(1)−O(1)	88.00(6)
O(5)#1−Cd(1)−O(1W)	89.85(6)	O(1W)−Cd(1)−O(1)	86.24(6)
N(1)−Cd(1)−O(1W)	89.72(6)	O(2)-Cd(1)−O(1)	52.77(5)
N(2)−Cd(1)−O(1W)	171.82(6)	O(5)#1−Cd(1)−O(6)#1	53.33(5)
O(5)#1−Cd(1)−O(2)	83.35(5)	N(1)−Cd(1)−O(6)#1	86.30(6)
N(1)−Cd(1)−O(2)	136.35(6)	N(2)−Cd(1)−O(6)#1	96.73(7)
N(2)−Cd(1)−O(2)	90.35(7)	O(1W)−Cd(1)−O(6)#1	89.90(6)
O(1W)−Cd(1)−O(2)	81.54(6)	O(2)−Cd(1)−O(6)#1	135.95(5)
O(5)#1−Cd(1)−O(1)	136.05(5)	O(1)−Cd(1)−O(6)#1	169.73(5)

Symmetry code: #1 x, $y + 1$, z

Table S6. Selected bond distances (Å) and angles (°) for complex **6**

Co(1)−O(5)#1	2.0129(18)	Co(1)−N(1)	2.142(2)
Co(1)−O(6)#2	2.0299(19)	Co(1)−N(2)#3	2.153(2)
Co(1)−O(1)	2.095(2)	Co(1)−O(2)	2.409(2)
O(5)#1−Co(1)−O(6)#2	123.41(8)	O(1)−Co(1)−N(2)#3	95.86(9)
O(5)#1−Co(1)−O(1)	147.67(8)	N(1)−Co(1)−N(2)#3	173.39(9)
O(6)#2−Co(1)−O(1)	88.90(8)	O(5)#1−Co(1)−O(2)	90.37(7)
O(5)#1−Co(1)−N(1)	87.66(8)	O(6)#2−Co(1)−O(2)	145.98(7)
O(6)#2−Co(1)−N(1)	93.17(9)	O(1)−Co(1)−O(2)	57.54(7)
O(1)−Co(1)−N(1)	89.63(9)	N(1)−Co(1)−O(2)	92.05(8)
O(5)#1−Co(1)−N(2)#3	85.74(8)	N(2)#3−Co(1)−O(2)	87.80(8)
O(6)#2−Co(1)−N(2)#3	90.63(9)		

Symmetry code: #1 $x + 1$, y, z; #2 $-x$, $-y$, $-z + 1$; #3 x, $y + 1$, $z - 1$

Table S7. Selected bond distances (Å) and angles (°) for complex **7**

Ni(1)−O(3)	1.982(3)	Ni(1)−O(2)	2.125(3)
Ni(1)−N(1)	2.086(4)	Ni(1)−O(1)	2.148(3)
Ni(1)−N(2)#1	2.109(4)	N(1)−Ni(1)−O(1)	88.25(14)
O(3)−Ni(1)−N(1)	89.72(15)	N(2)#1−Ni(1)−O(1)	89.90(14)
O(3)−Ni(1)−N(2)#1	92.49(15)	O(2)−Ni(1)−O(1)	61.72(12)
N(1)−Ni(1)−N(2)#1	177.76(16)	N(2)#1−Ni(1)−O(2)	91.78(15)
O(3)−Ni(1)−O(2)	92.85(13)	O(3)−Ni(1)−O(1)	154.53(14)
N(1)−Ni(1)−O(2)	88.48(14)		

Symmetry code: #1 $-x + y + 2/3, -x + 1/3, z + 1/3$

Table S8. Selected bond distances (Å) and angles (°) for complex **8**

Cu(1)−O(1)#1	1.928(5)	Cu(1)−N(1)	1.999(7)
Cu(1)−O(1)	1.928(5)	Cu(1)−N(1)#1	1.999(7)
O(1)#1−Cu(1)−O(1)	153.7(3)	O(1)#1−Cu(1)−N(1)#1	91.1(3)
O(1)#1−Cu(1)−N(1)	91.2(2)	O(1)−Cu(1)−N(1)#1	91.2(2)
O(1)−Cu(1)−N(1)	91.1(3)	N(1)−Cu(1)−N(1)#1	170.0(4)

Symmetry code: #1 $x - y, -y, -z - 1/2$

Table S9. Selected bond distances (Å) and angles (°) for complex **9**

Zn(1)−O(1)	1.8530(13)	Zn(1)−N(1)	2.1656(16)
Zn(1)−O(6)#1	1.9771(13)	Zn(1)−O(4)#2	2.1814(15)
Zn(1)−O(3)#2	2.1445(14)	O(6)#1-Zn(1)-O(4)#2	94.76(6)
O(1)−Zn(1)−O(6)#1	107.09(6)	O(3)#2−Zn(1)−O(4)#2	62.39(5)
O(1)−Zn(1)−O(3)#2	132.36(6)	N(1)−Zn(1)−O(4)#2	145.61(7)
O(6)#1−Zn(1)−O(3)#2	111.48(6)	O(3)#2−Zn(1)−N(1)	91.31(5)
O(1)−Zn(1)−N(1)	95.74(6)	O(1)−Zn(1)−O(4)#2	87.94(6)
O(6)#1−Zn(1)−N(1)	116.43(6)		

Symmetry code: #1 $-x + 1, -y - 1, -z + 1$; #2 $x, -y - 3/2, z - 1/2$

Table S10. Selected bond distances (Å) and angles (°) for complex **10**

Cd(1)−N(2)	2.335(3)	Cd(1)−Cl(1)#1	2.5619(10)
Cd(1)−N(1)	2.344(3)	Cd(1)−Cl(1)	2.5779(10)
Cd(1)−O(1)	2.352(2)	N(2)−Cd(1)−Cl(1)	89.36(7)
Cd(1)−O(2)	2.397(2)	N(2)−Cd(1)−N(1)	173.30(10)
N(2)−Cd(1)−O(1)	85.69(9)	N(1)−Cd(1)−Cl(1)	87.85(7)
N(1)−Cd(1)−O(1)	88.68(9)	O(1)−Cd(1)−Cl(1)	98.22(6)
N(2)−Cd(1)−O(2)	93.78(9)	O(2)−Cd(1)−Cl(1)	152.97(6)
N(1)−Cd(1)−O(2)	85.99(9)	Cl(1)#1−Cd(1)−Cl(1)	119.91(4)
O(1)−Cd(1)−O(2)	55.38(8)	O(1)−Cd(1)−Cl(1)#1	141.82(6)
N(2)−Cd(1)−Cl(1)#1	92.37(7)	O(2)−Cd(1)−Cl(1)#1	86.82(6)
N(1)−Cd(1)−Cl(1)#1	94.31(8)		

Symmetry code: #1 $-x + y, -x - 1, z$

Table S11. Hydrogen bonding geometries (Å, °) of complexes **1**, **2**, **3**, **5**, **6** and **9**

Complex	D–H···A	D–H	H···A	D···A	D–H···A
1	N4–H4A···O6	0.86	2.02	2.3717	171
2	O1W–H1WB···O5	0.85	2.29	2.7466	113
3	N3–H3B···O4	0.86	2.11	2.8978	151
5	O1W–H1WA···O6	0.85	2.03	2.7369	141
6	O2W–H2WB···O1	0.85	2.17	2.9919	164
9	N2–H2B···O2	0.86	1.89	2.7271	166

Table S12. The R and R^2 values of peak currents *vs*. scan rates/square root of scan rates

Values	**1**-CPE	**2**-CPE	**3**-CPE	**6**-CPE	**7**-CPE	**8**-CPE
R (peak current *vs*. scan rate)	0.99598	0.99996	0.75330	0.99380	0.99894	0.98909
R^2 (peak current *vs*. scan rate)	**0.99198**	**0.99992**	0.56746	**0.98764**	**0.99788**	0.97830
R (peak current *vs*. square root of scan rate)	0.97941	0.98832	0.83659	0.97139	0.98707	0.99293
R^2 (peak current *vs*. square root of scan rate)	0.95924	0.97678	**0.69988**	0.94360	0.97431	**0.98591**

Note: R= correlation coefficient

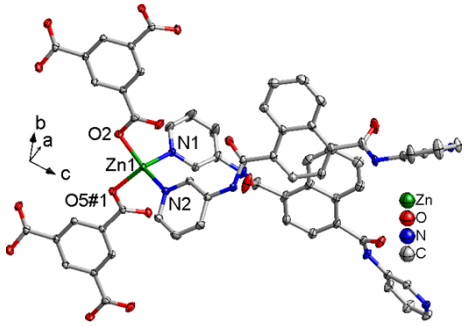

Fig. S1 ORTEP view of **4** showing the local coordination environment of the Zn(II) ion with hydrogen atoms omitted for clarity (50% probability displacement ellipsoids).

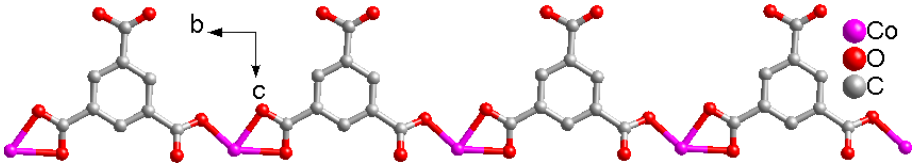

Fig. S2 The 1D $[Co(1,3,5\text{-}HBTC)]_n$ chain of complex **1**.

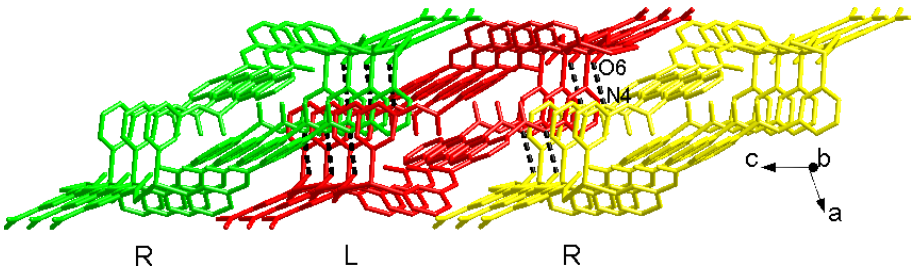

Fig. S3 View of 2D supramolecular architecture formed by N–H···O hydrogen-bonding interactions (H bonds: dotted line) in **1**.

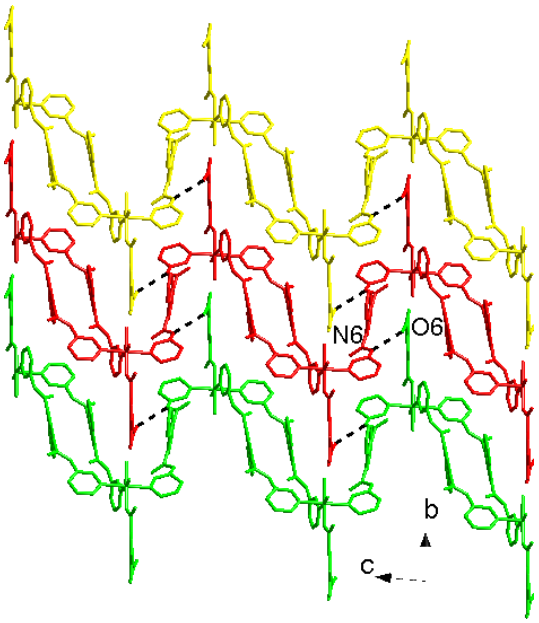

Fig. S4 View of 2D supramolecular architecture formed by hydrogen-bonding interaction in **2** (H bonds: dotted line).

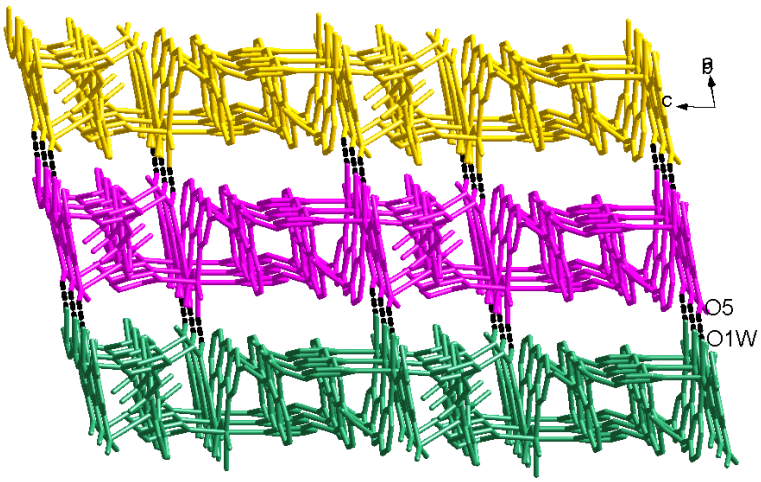

Fig. S5 View of 3D supramolecular architecture formed by hydrogen-bonding interaction in **2** (H bonds: dotted line).

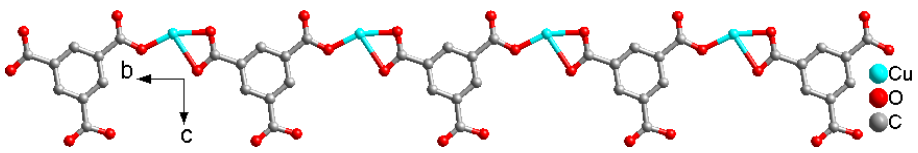

Fig. S6 The 1D $[Cu(1,3,5\text{-}HBTC)]_n$ chain of complex **3**.

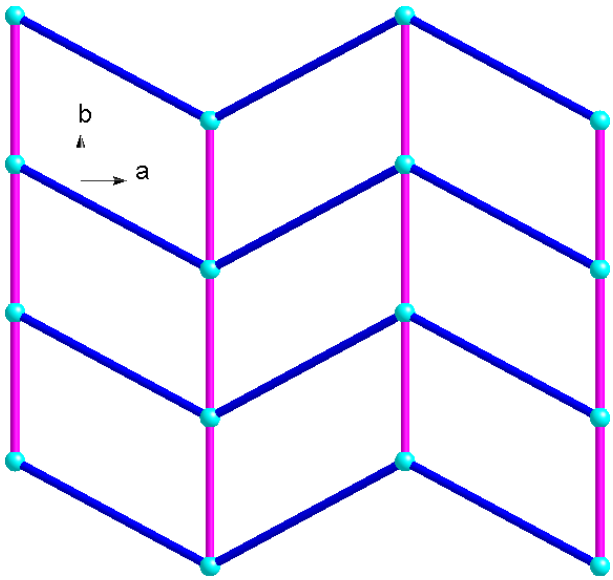

Fig. S7 Schematic representation of *sql* net in **3**.

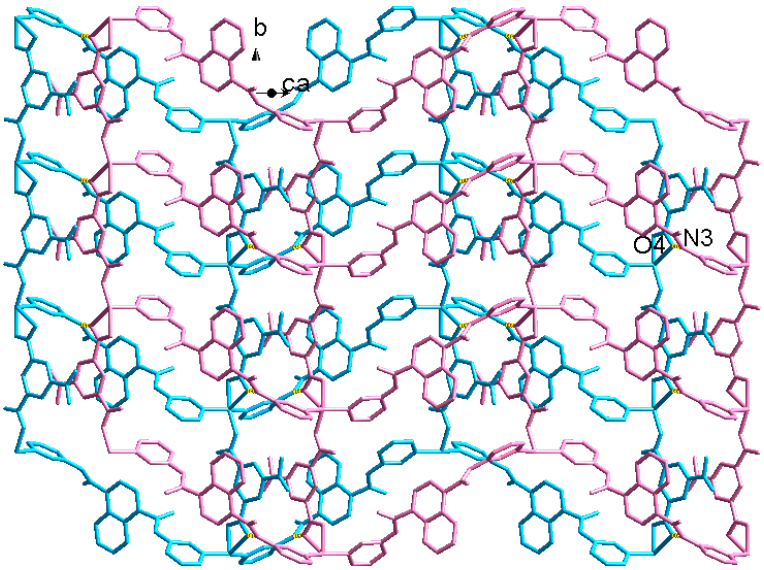

Fig. S8 View of 3D supramolecular architecture formed by hydrogen-bonding interaction in **3** (H bonds: dotted line).

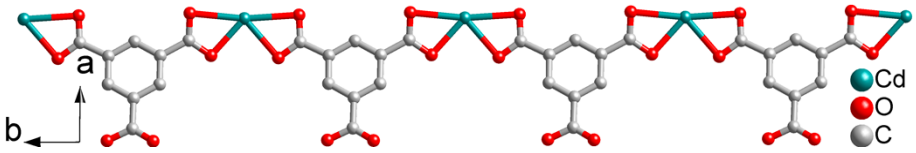

Fig. S9 The 1D $[Cd(1,3,5\text{-}HBTC)]_n$ chain of complex **5**.

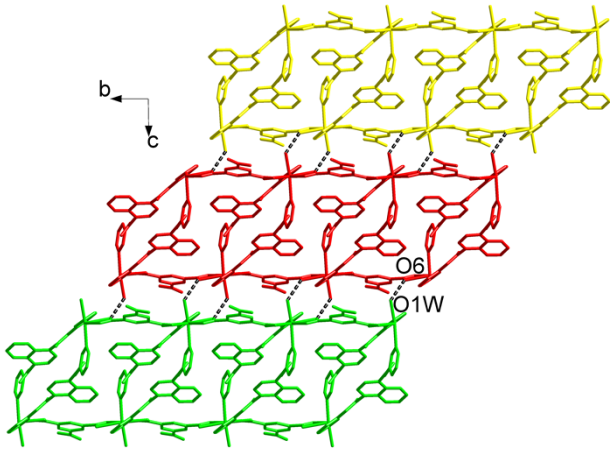

Fig. S10 View of 2D supramolecular architecture formed by hydrogen-bonding interaction in **5** (H bonds: dotted line).

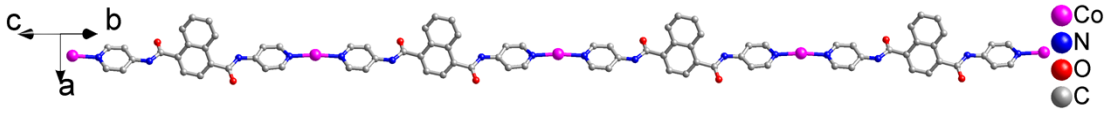

Fig. S11 The 1D $[Co(4\text{-}DPNA)]_n$ linear chain of complex **6**.

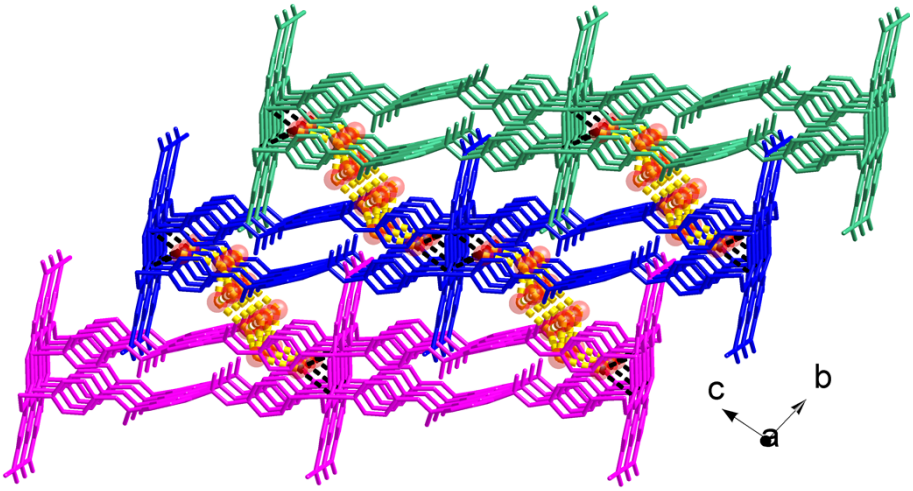

Fig. S12 View of 3D supramolecular architecture by hydrogen-bonding interaction in **6** (H bonds: dotted line).

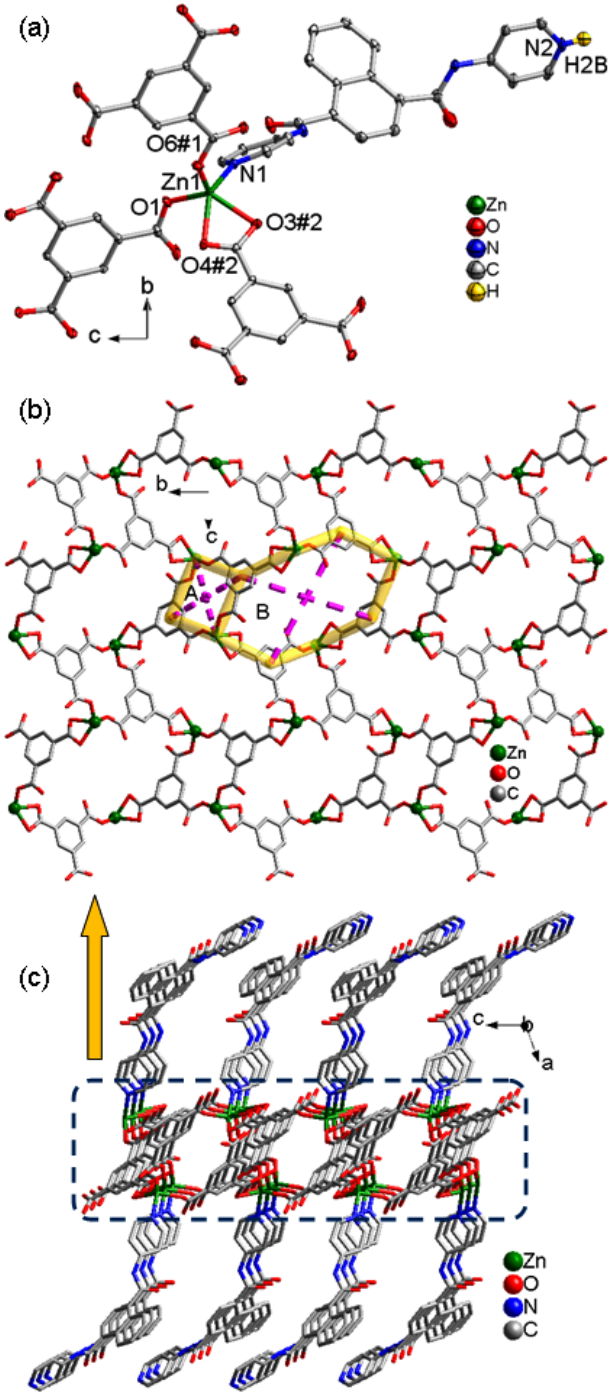

Fig. S13 (a) The coordination geometry of the Zn(II) ion in **9**. (b) View of the $[Zn\text{-}(1,3,5\text{-}BTC)]_n$ 2D network. (c) View of the 2D network of complex **9** with 4-Hdpna hanging on the $[Zn\text{-}(1,3,5\text{-}BTC)]_n$ 2D network.

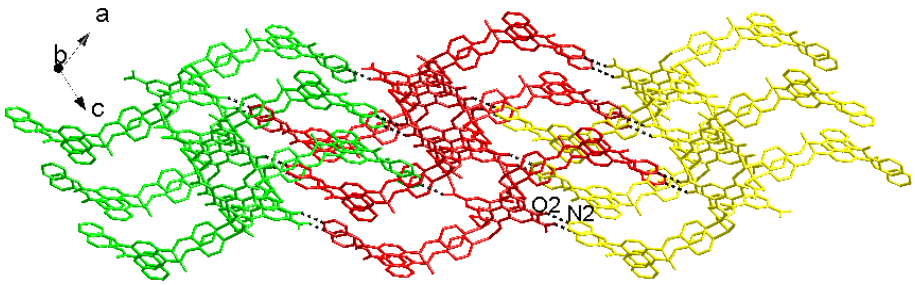

Fig. S14 View of 3D supramolecular architecture formed by hydrogen-bonding interaction in **9** (H bonds: dotted line).

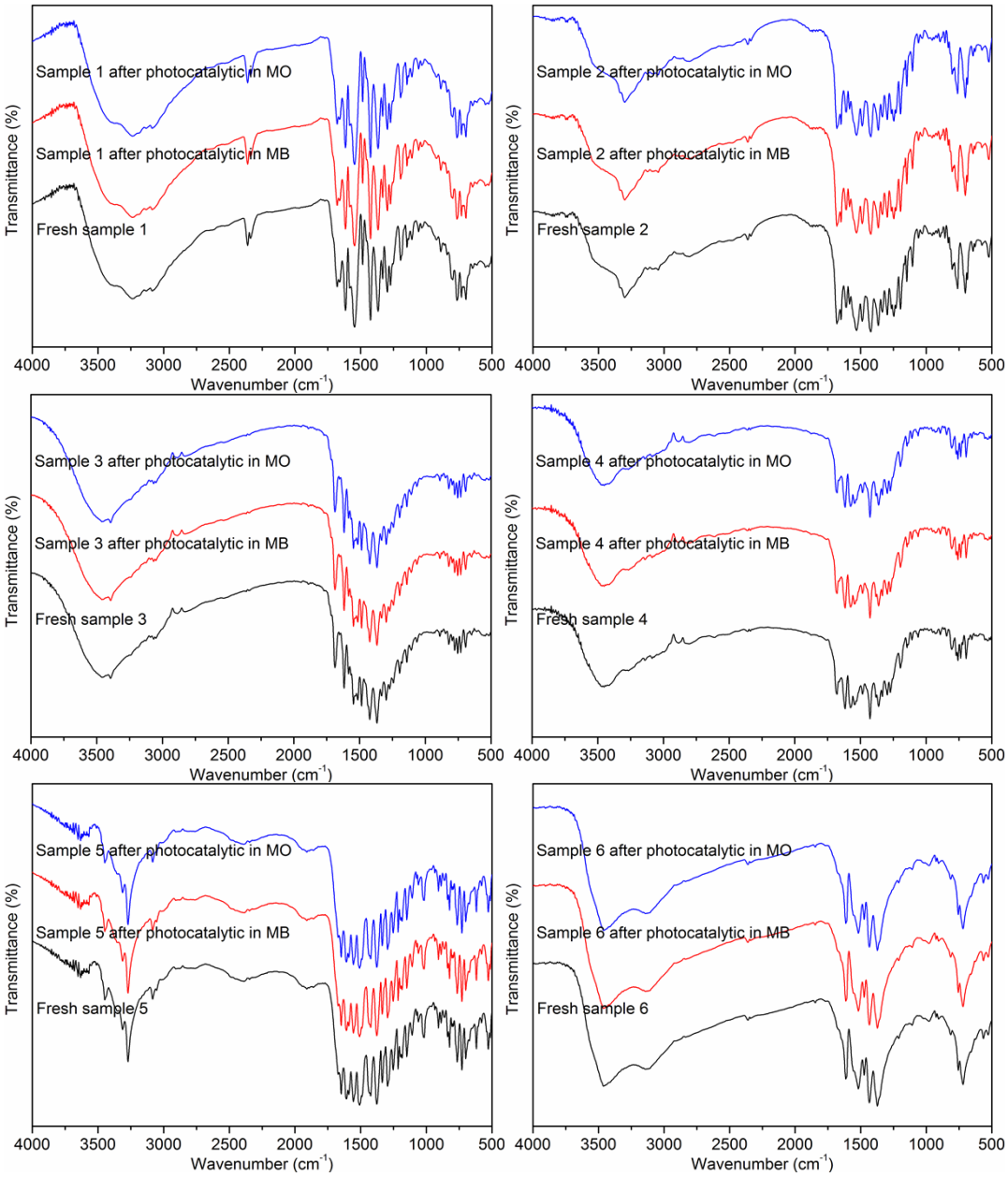

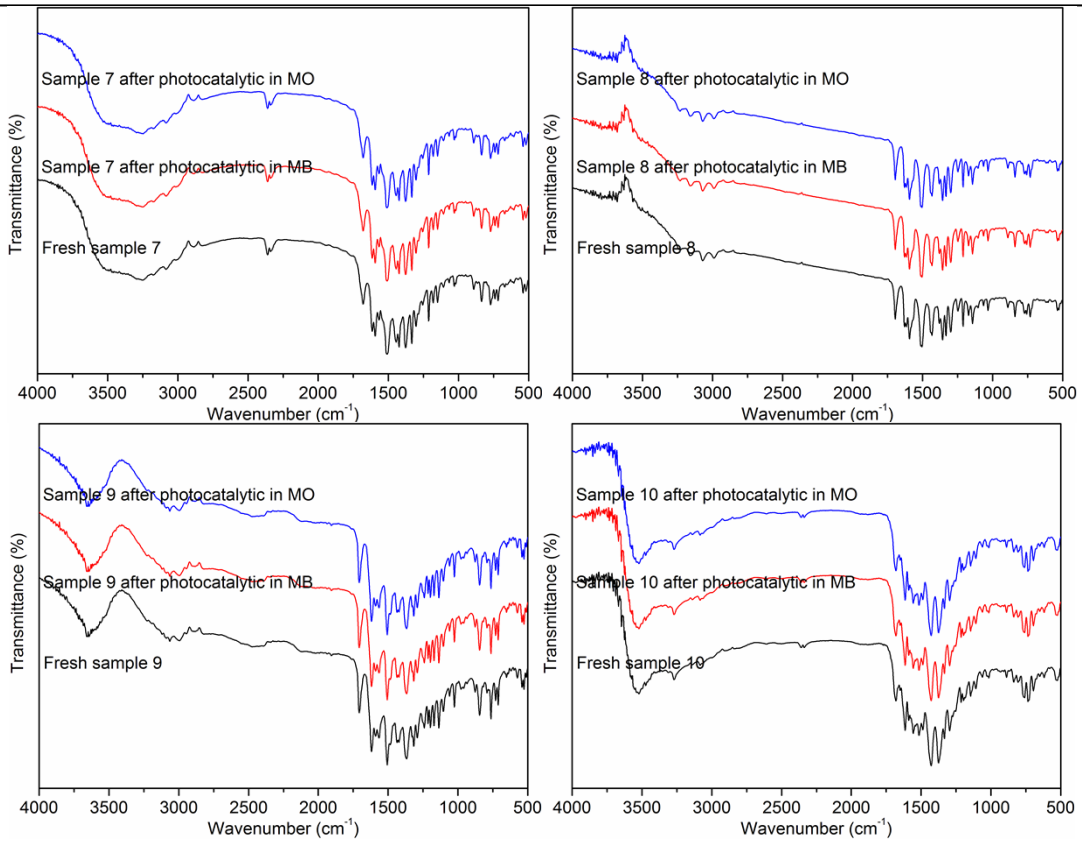

Fig. S15 The IR spectra of complexes **1**–**10**.

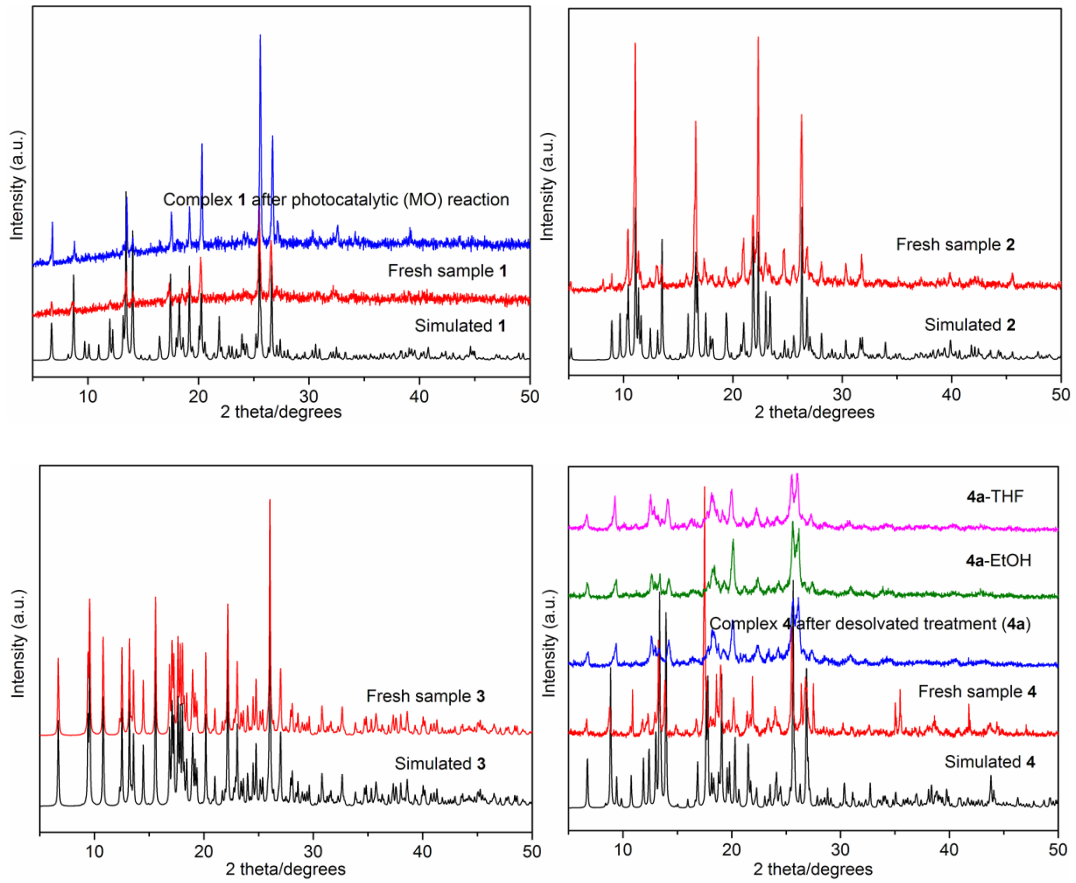

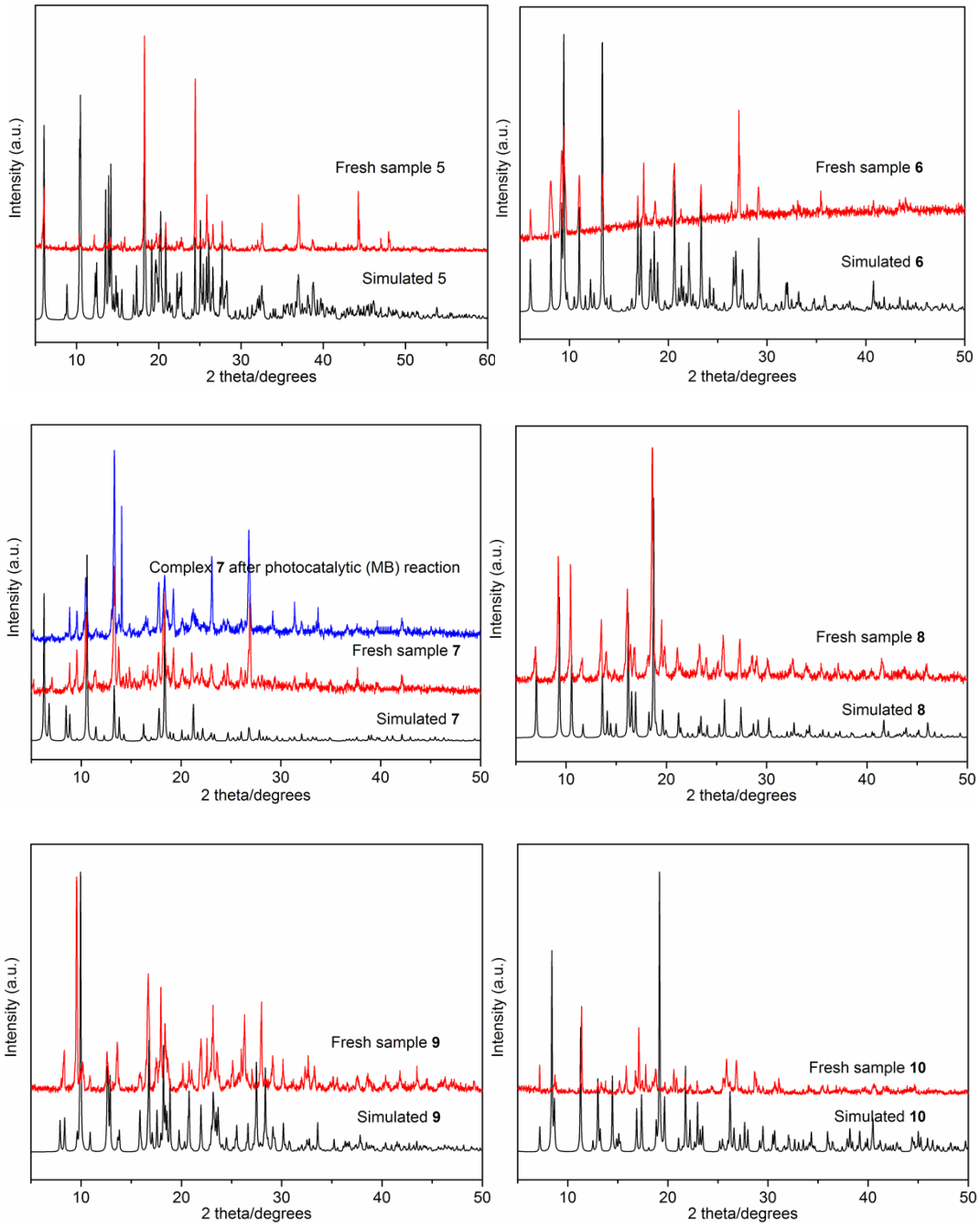

Fig. S16 The powder X-ray diffraction patterns of simulated and fresh samples, as well as some of those after photocatalysis or solvent exchange for complexes **1**–**10**.

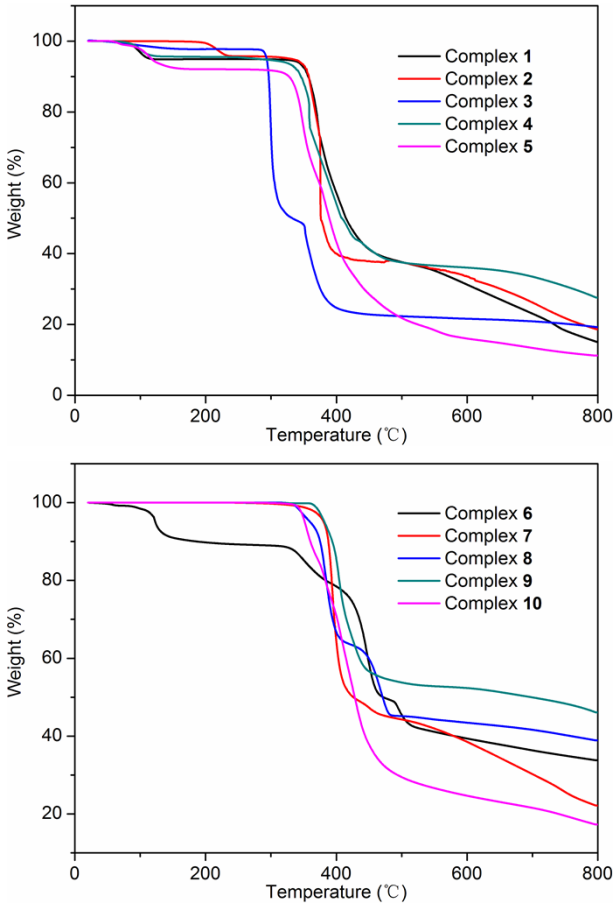

Fig. S17 The TG curves of complexes **1**–**10**.

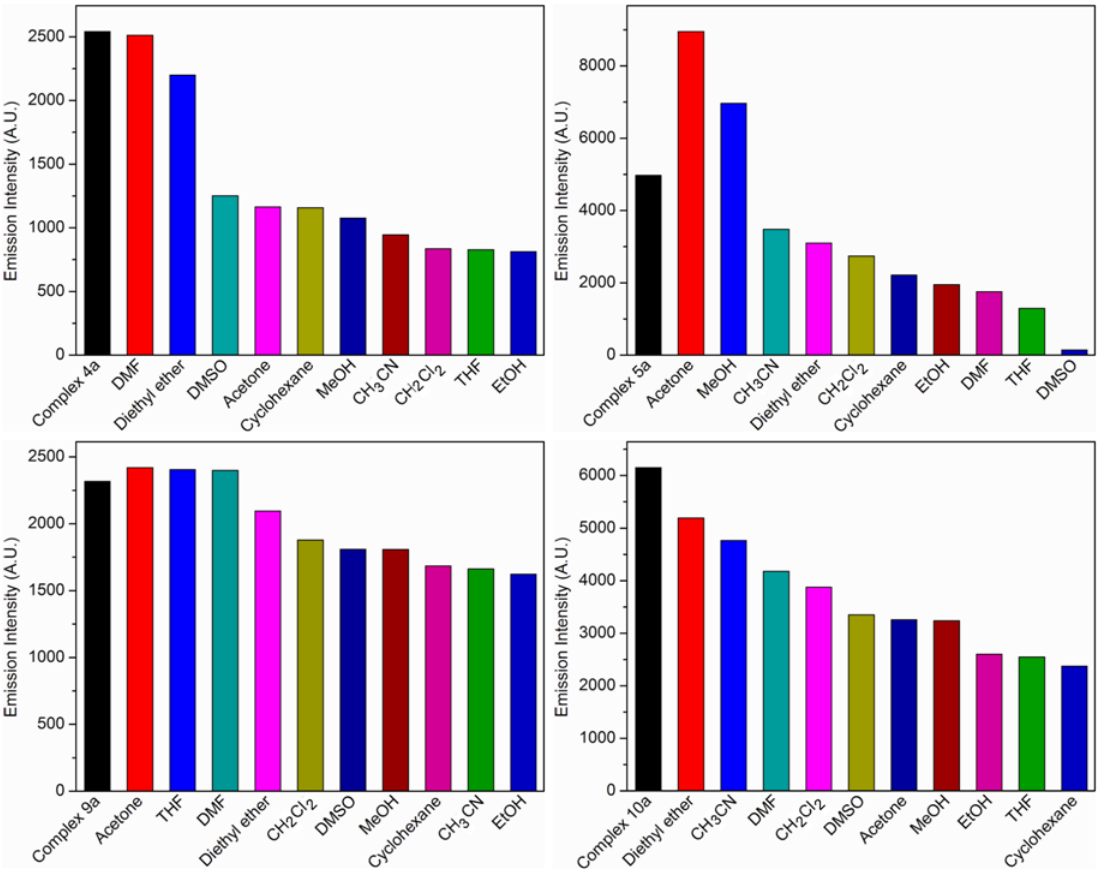

Fig. S18 Fluorescence intensity histograms of **4a**-, **5a**-, **9a**- and **10a**-solvents.

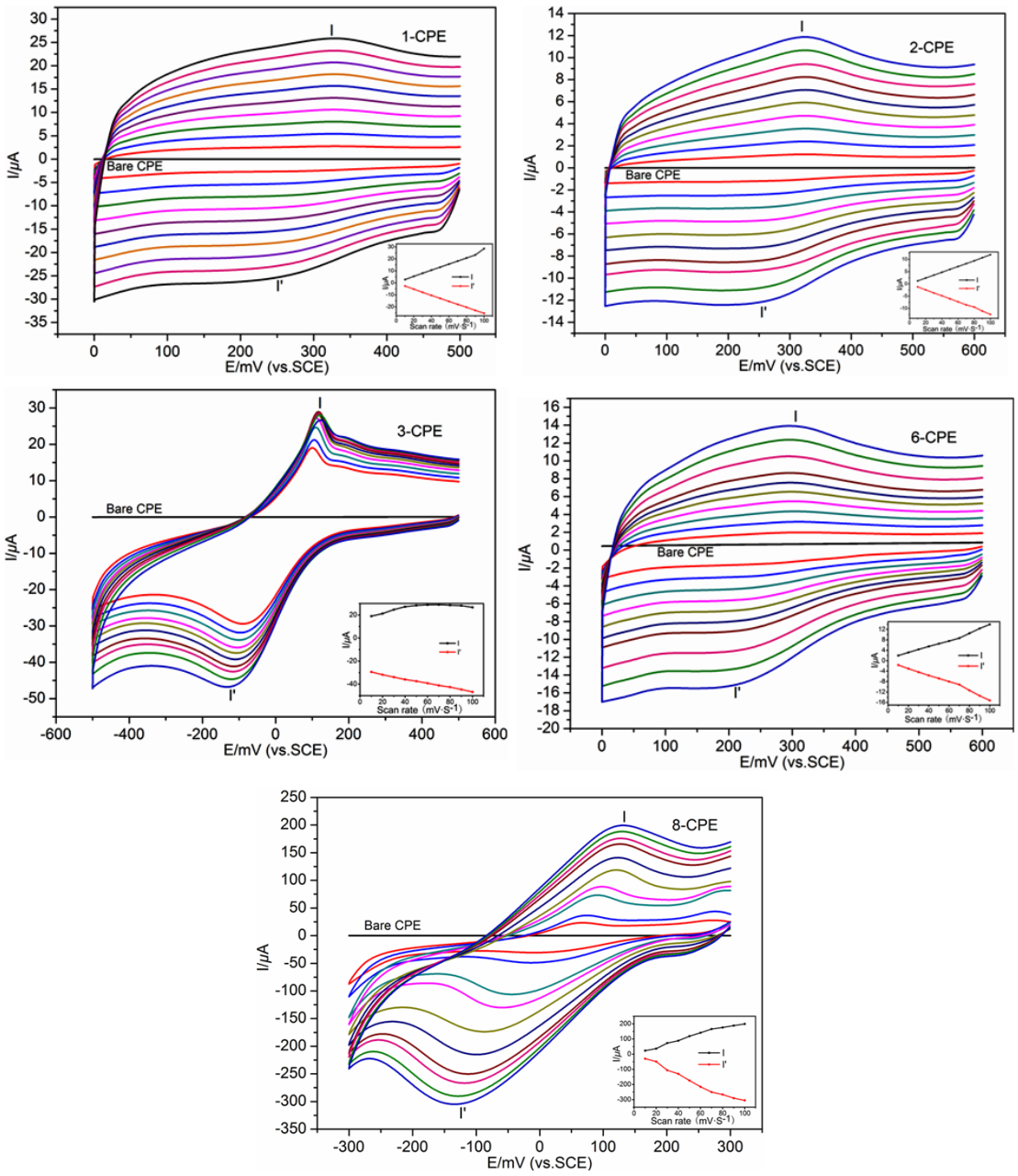

Fig. S19 Cyclic voltammograms of the **1**-, **2**-, **3**-, **6**-, **8**-CPE in 0.01 M H_2SO_4 + 0.5 M Na_2SO_4 aqueous solution at different scan rates (from inner to outer: 10, 20, 30, 40, 50, 60, 70, 80, 90, 100 mV·s-1). The inset shows the plots of the anodic and cathodic peak currents against scan rates.

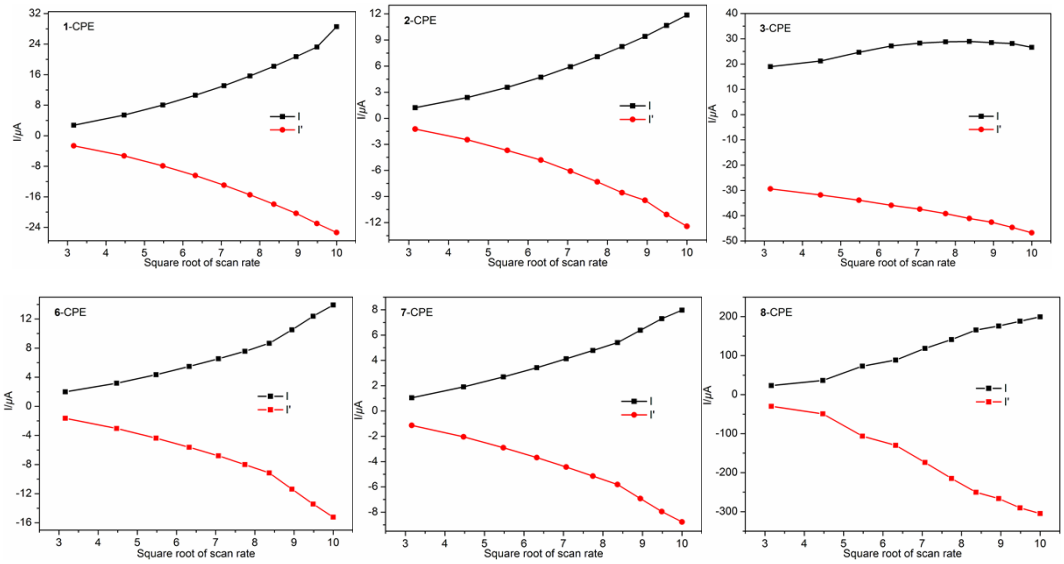

Fig. S20 The plots of the anodic and cathodic peak currents against square root of scan rates.

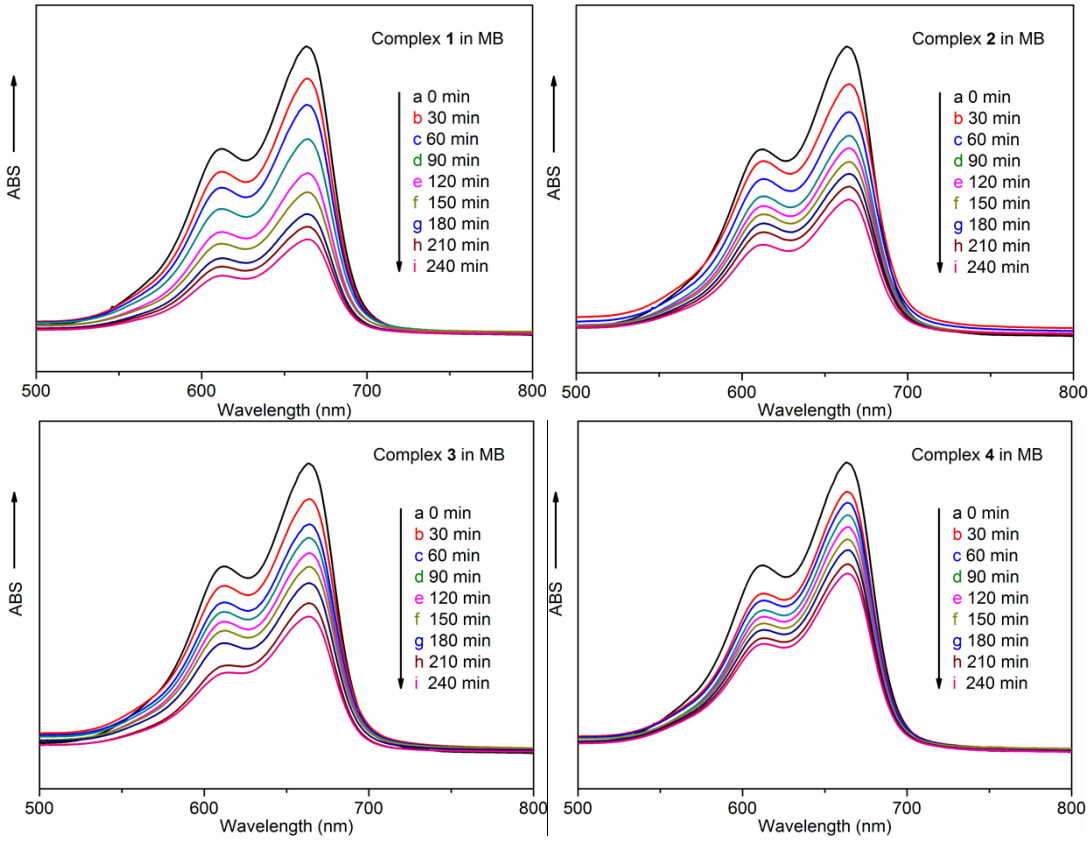

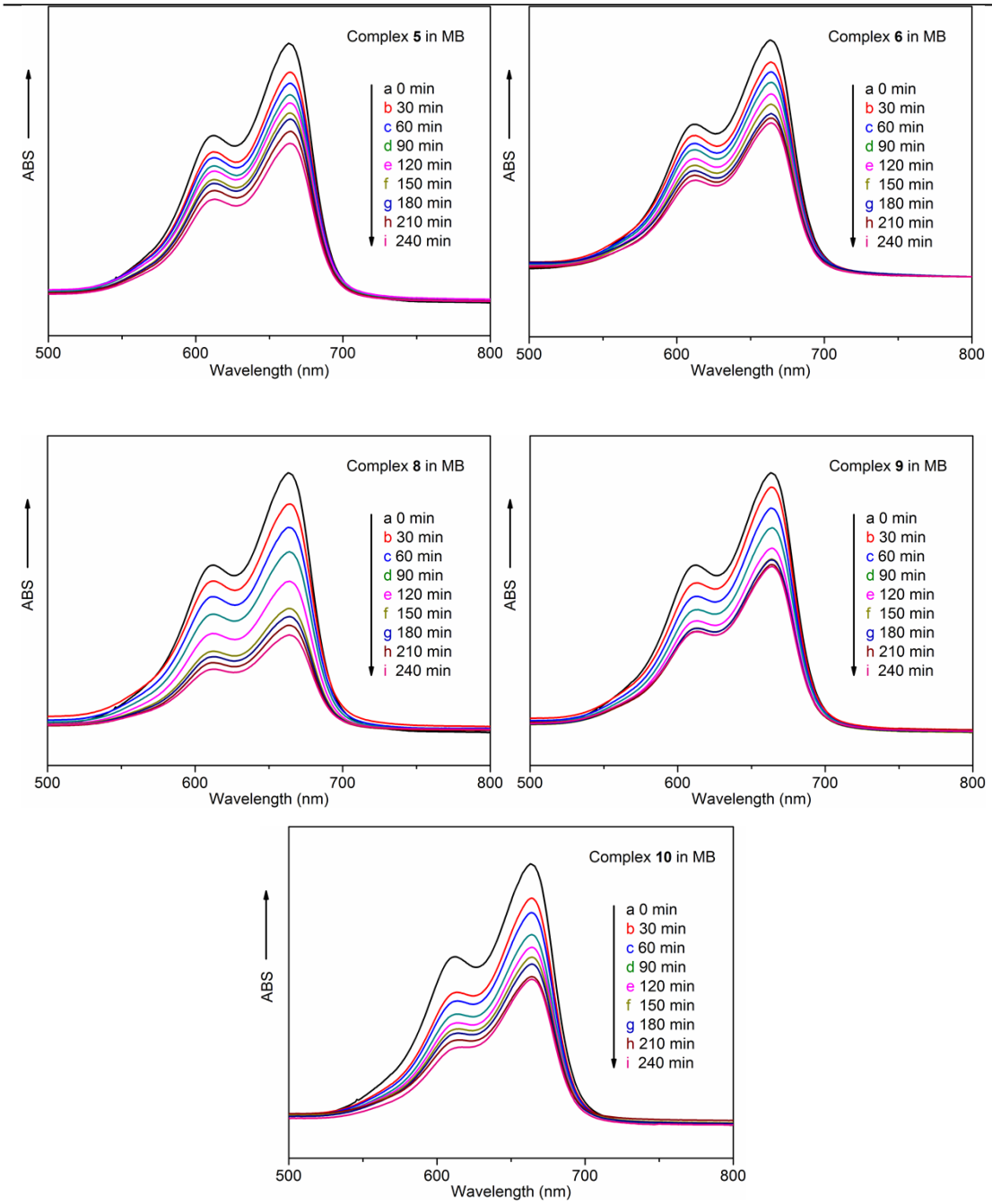

Fig. S21 Absorption spectra of the MB solution during the decomposition reaction under UV irradiation with the presence of complexes **1**−**6** and **8**−**10**.

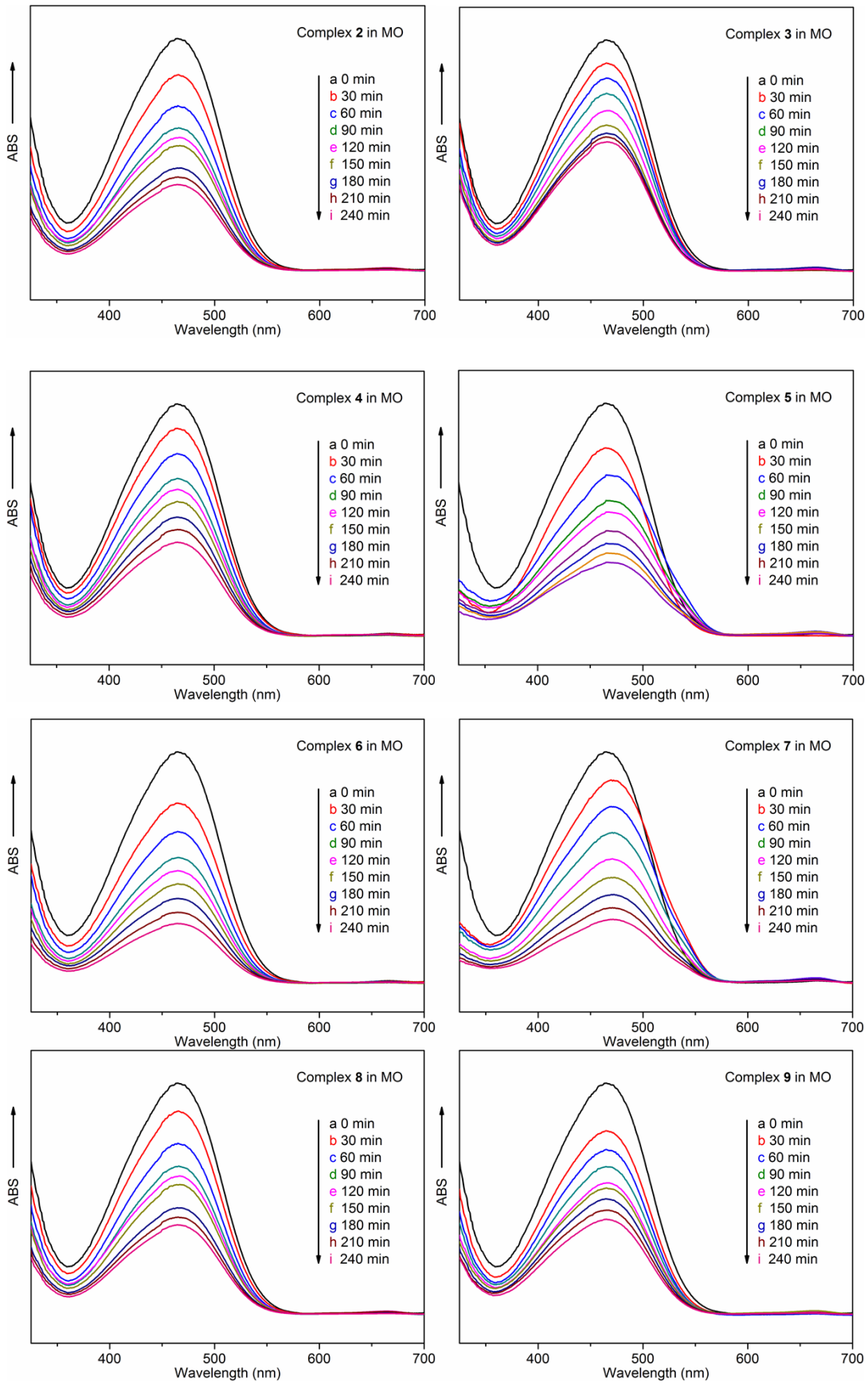
Complex 2 in MO
Complex 3 in MO
Complex 4 in MO
Complex 5 in MO
Complex 6 in MO
Complex 7 in MO
Complex 8 in MO
Complex 9 in MO
a 0 min
b 30 min
c 60 min
d 90 min
e 120 min
f 150 min
g 180 min
h 210 min
i 240 min
ABS
Wavelength (nm)
400
500
600
700

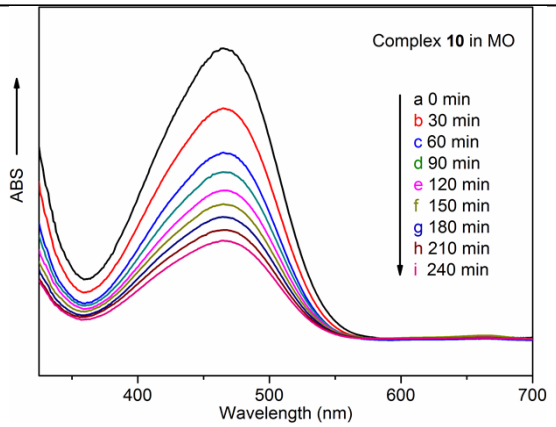

Fig. S22 Absorption spectra of the MO solution during the decomposition reaction under UV irradiation with the presence of complexes **2**–**10**.